N73-26075

FEATURES OF THE KINEMATICS OF MANIPULATORS AND VOLUMES METHODS

I. B. Vinogradov, A. Ye. Kobrinskiy, Yu. A. Stepanenko, L. I. Tyves

ABSTRACT. A volumetric method of kinematic analysis of a manipulator which can be used in addition to the conventional trajectory method is presented. An ideal manipulator, the influence of limitations on the angles of rotation of the manipulator, and a manipulator with limitations in all joints are discussed.

1. Introduction. Conventional methods of kinematic analysis of mechanisms permit investigating the kinematics of a manipulator for given laws of motion of all its drive links. The difficulties caused by the great many degrees of system mobility are purely technical in nature. However, this approach, based on the study of particular trajectories of motion, tells nothing of the general kinematic properties of the manipulator. This makes it desirable to use another method, the volumetric method, along with the trajectory method of kinematic analysis for it permits obtaining general, integral evaluations of the kinematic properties of the manipulator characterizing some of its qualities when developing a set of trajectories.

A manipulator can function in a working space determined by the length of its links and the movements in its joints. The manipulator tongs can reach any point in this space, but the functional potentials of the mechanisms differ at different points. That is, inherent in the particular manipulator are definite properties characterizing the potential for performing different working operations at each point in the working space. Investigation of these working space properties, imparted by the manipulator, provides the means for evaluating important kinematic characteristics of the manipulator as a unit.

When the manipulator is at work it must be able to orient and move the tongs in different ways relative to the object of manipulation. However, structural and design limitations prevent moving the tongs to any point in the working space at any angle. Some solid angle, ψ, within which the tongs can be brought to this point, can be determined for each point in the space. Let us call angle ψ the spatial servicing angle, or the service angle. Let us call the relationship

$$\psi/4\pi = \Theta \qquad (1)$$

the service factor at a particular point. Some scalar field thus can be

established above the working space, or, putting it another way, each point in the space is set up in accordance with its service factor. The factor can change from 0 for points on the boundary of the working space to 1 for points in the so-caleed 100%, or full service, zone. It is technically justified to characterize the quality of the manipulator as a whole by the mean magnitude of the service factor, $\overline{\Theta}$, in the working space, dV

/6

$$\overline{\Theta} = \frac{1}{V}\int_{(V)} \Theta dV,$$

which can be called the full servicing factor, or the manipulator service.

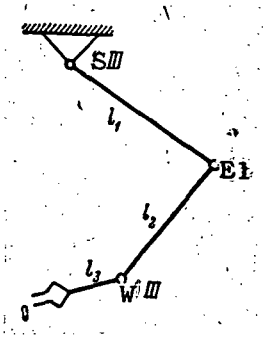

Figure 1.

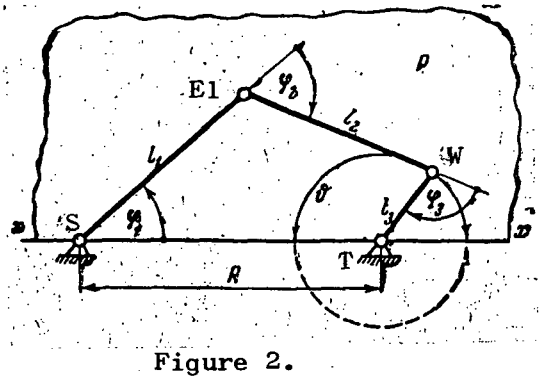

Figure 2.

In determining the magnitude of the service factor at the particular point, let us submit that the manipulator has gripped some object of negligibly small size located at this point with the jaws of the tongs. Let us now assume that the tongs can be moved, changing their orientation in the space, but that the object does not leave the particular point. At the same time, the coupling superposed on the manipulator by the object is similar to the coupling superposed by the ball joint located at the point of interest to us and coupling the tongs and the support. The manipulator is, in this case, converted into a three-dimensional mechanism, and Θ now can be determined by the spatial angle through which the axis of the tongs can be turned. Thus, the task of determining Θ is reduced to investigating a family of three-dimensional mechanisms with several degrees of mobility. The relative mobility of the links is limited by mechanism dimensions and by the drive systems for the kinematic couples. Therefore, it is desirable first to examine the properties of the "ideal" manipulator without regard for design and structural factors. This is done in what follows by using the example of a manipulator with eight degrees of freedom and one degree

of maneuverability [1]. A general algorithm for determining the volumetric kinematic properties in the case of arbitrary limitations on movements in the kinematic couplings then is presented.

2. The ideal manipulator. We will understand the ideal manipulator to be one with no limitations on movements in all kinematic couples, and in which the thicknesses of the links and the dimensions of the joints can be ignored.

Let us investigate the configuration of the service zones for an ideal manipulator with one degree of maneuverability (Figure 1). Its "arm" has Class III spherical turning couples in the "shoulder," and in the "wrist," and a Class V turning couple in the "elbow." We shall designate the kinematic couples by the first letter of the name of the corresponding joint in the human arm, and the degrees of freedom in the particular couple by Roman numerals. Let us designate the lengths of the links as l_1, l_2, l_3. The manipulator under consideration has one degree of maneuverability. The process of arbitrary reorientations of the tongs can be represented as the rotation of link WT with respect to fixed point T such that the trajectories of point W will lie in a sphere of radius l_3. The result is a three-dimensional 4-link mechanism with support ST (Figure 2). All links in this mechanism can be located in a single plane, P, the base plane, and can be rotated in turn around an axis passing through points S and T. Let us designate this axis x. In this case, point W will describe a circle in plane P and, together with plane P, a spherical surface around point T. Thus, investigation of the service provided by a 3-link manipulator with eight degrees of freedom can be reduced to the investigation of a series of flat 4-link closed mechanisms that differ by the length of the ST link. At the same time, the service factor for any point on the x-axis and, by changing the position of the x-axis in the space, for any point in the working space, can be determined. The Θ values for points on the x-axis will not depend on the position of the x-axis in space for the ideal manipulator being investigated so, it is sufficient to investigate one arbitrary position of this axis. Angles φ_1, φ_2, and φ_3 characterize the relative positions of the links.

/7

The movement of point T along x in the direction of the shoulder, S, as well as away from it, it limited by two maxima corresponding to the two limit positions of the mechanism. In one, the tongs are at the maximum distance from the shoulder

and point T will be at a distance from point S equal to $R_{max} = l_1 + l_2 + l_3$. In the other, angle φ_2 is maximum and the tongs are at the greatest distance from the first limit position.

Let us determine the configuration of the manipulator service zones. Known crankability conditions [2] provide the first zone, the full service zone. This zone is in the limits $l_1 + l_2 - l_3 \geq R \geq l_1 - l_2 + l_3$. when $l_1 > l_2 > l_3$ Figure 2). The magnitude of the service, Θ, changes from 0 to 1 beyond the limits of this zone.

The second zone is the limits $l_1 + l_2 + l_3 \geq R \geq l_1 + l_2 - l_3$, and

$$\frac{l_3^2 + R^2 - (l_1 + l_2)^2}{2Rl_3} = \cos\vartheta. \tag{2}$$

is valid.

Here ϑ is the maximum angle, read from the x-axis (see Figure 2), within which link l_3 can turn for a given R value. We shall call angle ϑ the service angle in the base plane. The manipulator can occupy positions symmetrical relative to the x-axis, so we shall take it that angle ϑ can change from 0 to π. The boundaries of the second zone correspond precisely to these limit values of ϑ.

The equality

$$\frac{l_3^2 + R^2 - (l_1 - l_2)^2}{2Rl_3} = \cos\vartheta, \tag{3}$$

is valid for the third zone, and

$$l_1 - l_2 + l_3 \geqslant R \geqslant l_1 - l_2 - l_3. \tag{4}$$

If the manipulator links are matched with the inequality $l_2 > l_1 > l_3$, the limits, using Eq. (3) when ϑ is equal to 0 and π, will be

$$l_2 - l_1 + l_3 \geqslant R \geqslant l_2 - l_1 - l_3. \tag{5}$$

Combining Eqs. (4) and (5), we obtain

$$|l_1 - l_2| + l_3 \geqslant R \geqslant |l_1 - l_2| - l_3.$$

Eqs. (2) and (3) provide angle ϑ for points along the x-axis. On the other hand, angle ϑ uniquely determines the spatial servicing angle, ψ, and the service factor Θ. There is a spherical sector in space corresponding to angle ϑ in the /8

base plane. The area of its spherical surface is determined by

$$F = 2\pi l_3^2 (1 - \cos\vartheta).$$

In accordance with the service factor definition, Eq. (1), we obtain

$$\Theta = \frac{2\pi l_3^2 (1 - \cos\vartheta)}{4\pi} = \frac{1 - \cos\vartheta}{2}. \tag{6}$$

Excluding ϑ from Eqs. (2) and (3), and solving for Θ, we obtain:

for the first zone

$$\Theta = 1; \tag{7}$$

for the second zone

$$\Theta = \frac{(l_1 + l_2)^2 - (R - l_3)^2}{4Rl_3}; \tag{8}$$

for the third zone

$$\Theta = \frac{(R + l_3)^2 - (l_1 - l_2)^2}{4Rl_3}. \tag{9}$$

Eqs. (7), (8), and (9) can be used to plot a graph of change in Θ with movement of the tongs (point T) from R_{max} to R_{min} (Figure 3). It corresponds to the $|l_1 - l_2| > l_3$ case, and has shown on it the limits of the zones differing by the nature of the change in Θ and considered above.

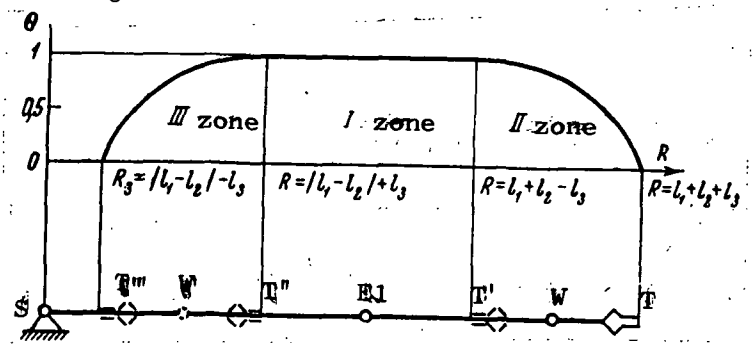

Figure 3.

Now let us consider the case when the manipulator length relationships yield $|l_1 - l_2| = l_3$. The distribution of the service zones now is completely subordinate to the previously obtained behavior patterns over the entire range of radius changes, except for the case when the tongs coincide with point S ($R = 0$). In this position, because of the rotation of the entire manipulator in the shoulder joint, the tongs can be oriented relative to point S in any manner, so $\Theta = 1$, and when $|l_1 - l_2| = l_3$, point S can be called a special point. There also are certain

special features present in the distribution of Θ in the third zone when $|l_1 - l_2| < l_3$. In particular, there is a sector in this zone with Θ = 1 (Figure 4). In accordance with Eq. (9), Θ = 1 when $R = R_1 = l_3 + |l_1 - l_2|$ and $R = R_2 = l_3 - |l_1 - l_2|$. Θ is a minimum when $R = R_3 = \sqrt{l_3^2 - (l_1 - l_2)^2}$. Thus when $R < R_2$ the tongs acquire a crankability (Figure 5) that is retained to R = 0. We obtain $R_1 = R_2 = R_3$ when $l_1 = l_2$ and we will have Θ = 1 on the Θ = f (R) graph (Figure 4) in the limits $l_1 + l_2 - l_3 \geq R \geq 0$. Obviously, $l_1 = l_2$ and $l_3 \to 0$ are, from the point of view of increase in service, the most advantageous link length relationships because Θ will be maximum. /9

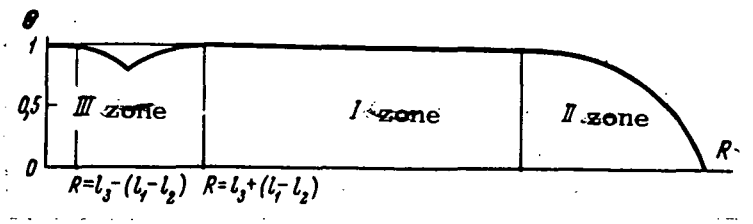

Figure 4.

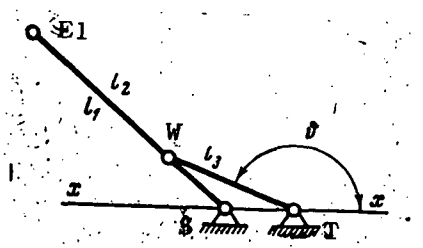

Figure 5.

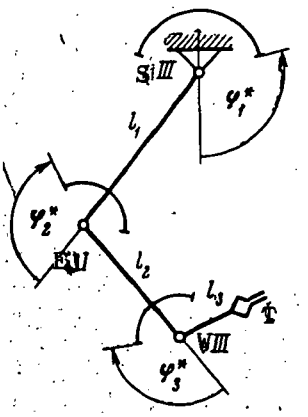

Figure 6.

3. <u>The influence of limitations.</u> Structural limitations on the angles of rotation of the manipulator links in all kinematic couples have a significant influence on manipulator volumetric properties. We shall designate the limiting values of the angles of rotation in the i^{th} joint φ_i^* (Figure 6). Here we shall consider the limitations on the angles of rotation of the links to the symmetrical with respect to the axes of the preceding links.

A. Let us examine the influence of limitation of angle φ_3, assuming that the limitations imposed on the remaining angles are $\varphi_2^* = \pi$, $\varphi_1^* = \pi$.

Let point T move from R_{max} to R_{min} (Figure 7). Here $\Theta = f(R)$ will be determined by a function of Eq. (8) until angle φ_3 reaches the boundary value $\varphi_3 = \varphi_3^*$. Radius R_1 will correspond to this value

$$R_1 = \sqrt{(l_1 + l_2)^2 + l_3^2 + 2l_3(l_1 + l_2)\cos\varphi_3^*}. \quad (10)$$

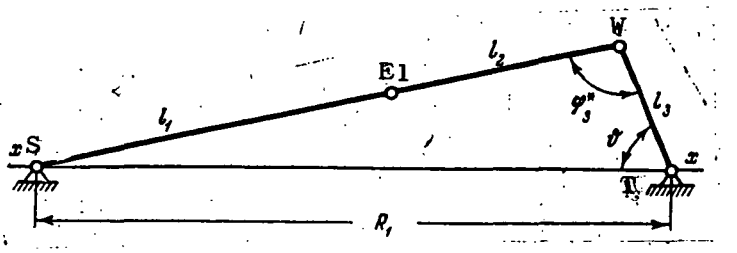

Figure 7.

Limitation φ_3^* influences the magnitude of the service angle, ϑ, when there is a further reduction in R, but this influence differs with different R values. Now ϑ can be depicted as the difference between two angles characterizing the limits in the position of link l_3 as it turns clockwise (α) and counterclockwise (β) (Figure 8). The manipulator under consideration has one degree of maneuverability so the values of α and β on only one side of the x-axis, that is, in the limits

$$0 \le \alpha \le \pi, \quad (11)$$

$$0 \le \beta \le \pi, \quad (12)$$

are of interest to us.

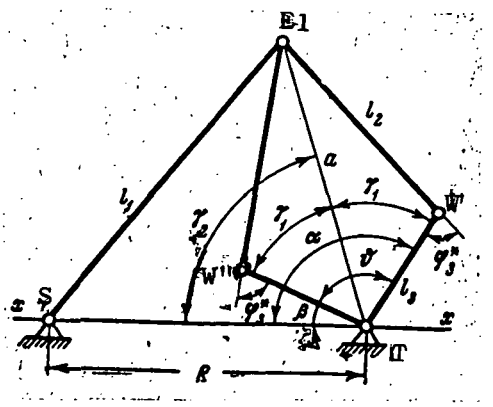

Figure 8.

Here the set of permissible wrist positions forms a ring on the surface of a sphere of radius l_3 and area $F = 2\pi l_3^2(\cos\beta - \cos\alpha)$, from whence

$$\Theta = \frac{\cos\beta}{2} - \frac{\cos\alpha}{2}. \quad /10$$

Let us examine change in $\cos\alpha$ and $\cos\beta$ as a function of R.

The limiting position for links l_2 and l_3 is angle α on the section $R_1 \ge R \ge R_{min}$. The links are positioned at angle φ_3^*. Angle α can be represented in the form of the sum of two angles, γ_1 and γ_2, determined by the equalities

3

$$\sin\gamma_1 = \frac{l_2}{a}\sin\varphi_3^*;$$

$$\cos\gamma_2 = \frac{a^2 + R^2 - l_1^2}{2aR};$$

$$a = \sqrt{l_2^2 + l_3^2 + 2l_2 l_3 \cos\varphi_3^*}.$$

After the transformations, we obtain

$$\cos\alpha = \cos(\gamma_1 + \gamma_2) = \pm\frac{a^2 + R^2 - l_1^2}{2a^2R}\sqrt{a^2 - l_2^2\sin^2\varphi_3^*} - \frac{l_2\sin\varphi_3^*}{2a^2R}\sqrt{4a^2R^2 - (a^2 + R^2 - l_1^2)^2}. \quad (13)$$

Let us put a "+" sign in front of the first term when $l_3 + l_2\cos\varphi_3^* \geq 0$ ($\gamma_1 \leq \pi/2$ corresponds to this), and a "-" sign when $l_3 + l_2\cos\varphi_3^* < 0$ (here, $\gamma_1 > \pi/2$).

Angle α increases with a decrease in R, reaching the value $\alpha = \pi$ when

$$R_2 = \sqrt{l_1^2 - l_2^2\sin^2\varphi_3^*} - l_2\cos\varphi_3^* - l_3.$$

Taking it that $R_2 \geq R \geq R_{min}$ in the zone, we have $\alpha > \pi$. In accordance with Eq. (11), we will conditionally consider $\alpha = \pi$.

Moving on to consideration of change in β as a function of R, we note that for small R values angle β depends only on the link length relationship, but also depends on φ_3^* when R values are large (Figure 9). Let us designate the boundary value of R separating these two regions R_3.

$$R_3 = \sqrt{l_3^2 + (l_1 - l_2)^2 - 2l_3(l_1 - l_2)\cos\varphi_3^*}.$$

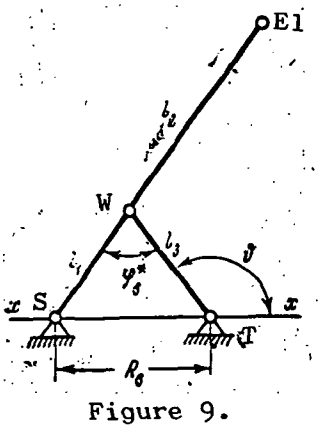

Figure 9.

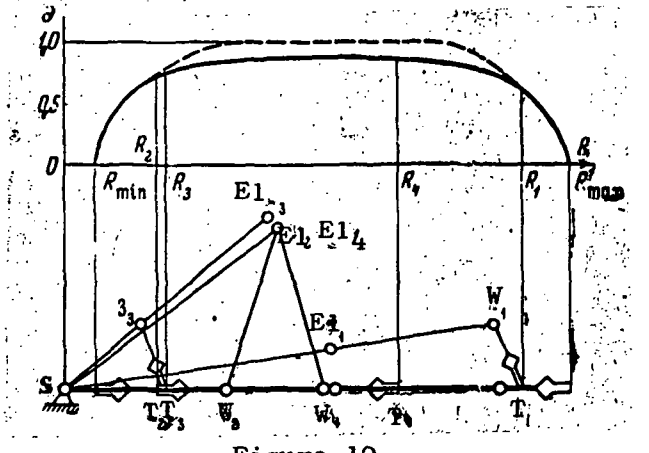

Figure 10.

The limiting position for links l_2 and l_3 is angle β on the section $R_1 \geq R \geq R_3$. The links are positioned at angle φ_3^*. Angle β can be represented in the form of the difference between angles $\gamma_2 - \gamma_1$ (Figure 8), so

$$\cos\beta = \cos(\gamma_2 - \gamma_1) = \pm\frac{a^2+R^2-l_1^2}{2a^2R}\sqrt{a^2 - l_2^2\sin^2\varphi_3^*} + \\ + \frac{l_2\sin\varphi_3^*}{2a^2R}\sqrt{4a^2R^2-(a^2+R^2-l_1^2)^2}.$$

Selection of the sign in front of the first term is determined in the same way as in Eq. (13).

Angle β decreases with increase in R, and equals zero when

$$R_4 = \sqrt{l_1^2 - l_2^2\sin^2\varphi_3^*} + l_2\cos\varphi_3^* + l_3.$$

We have $\beta < 0$ in the zone $R_{max} \geq R \geq R_4$ so, in accordance with Eq. (12), we will conditionally take $\beta = 0$ for this zone.

Limitation φ_3^* has no influence on manipulator movement near R_{min}, when $R_2 \geq R \geq R_{min}$ and $R_3 \geq R \geq R_{min}$ (given the condition that $|l_1 - l_2| \geq l_3$) and $\Theta = f(R)$ is determined from Eq. (9).

Figure 10 shows change in the service factor for the different zones. Shown are Θ values for the ideal manipulator (dashed curve) and the characteristic positions of the manipulator in each of the zones.

B. Let us now investigate the influence of the limitation on angle φ_2. Let us put $\varphi_2^* \leq \varphi_2 \leq \varphi_2^*$; $\varphi_3^* = \pi$; $\varphi_1^* = \pi$. As in the preceding case there are several characteristic zones in the range of changes in radius R from R_{min} to R_{max}. Let us first consider the zone near R_{min}. Figure 11 shows the position of the manipulator in this zone when $\varphi_2 = \varphi_2^*$. From triangle SWT we have

$$R = \sqrt{l_1^2 + l_2^2 + 2l_1l_2\cos\varphi_2^* - l_3^2\sin^2\theta} - l_3\cos\theta.$$

Using Eq. (6), we find

$$\theta = \frac{(R+l_3)^2 - (l_1^2 + l_2^2 + 2l_1l_2\cos\varphi_2^*)}{4Rl_3}.$$

This expression is valid when $R_1 \geq R \geq R_{min}$, where boundary R_1 can be determined from (see Figure 12) /12

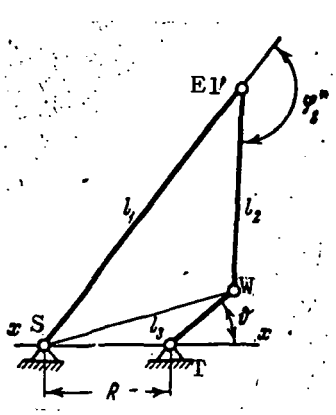

Figure 11.

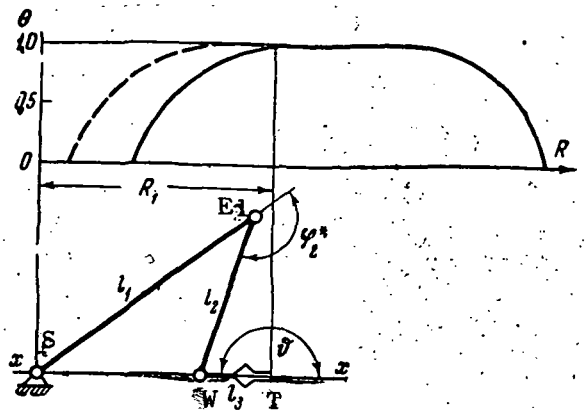

Figure 12.

Angle φ_2 always will be less than φ_2^* for the larger values of radius R, so the Θ distribution will be what it is for the ideal manipulator. Figure 12 shows $\Theta = f(R)$ for the φ_2 limitation. The solid line shows the function $\Theta = f(R)$ for a manipulator with the φ_2^* limitation, and the dashed line that for the ideal manipulator. Thus, if the φ_3 limitation influenced the Θ distribution at all points in the working space, reducing the service magnitude as compared to the ideal manipulator, the φ_2 limitation reduces the service factor only near the shoulder.

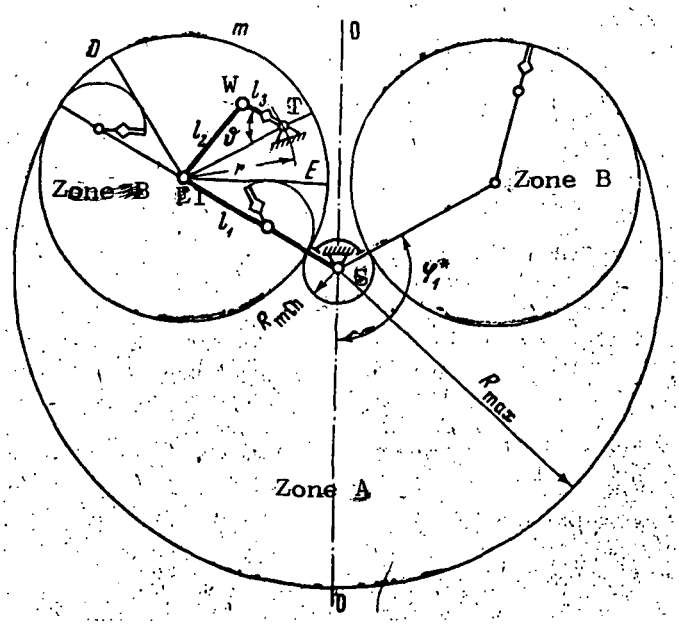

Figure 13.

C. Let us examine the case when $\varphi_1^* \leq \varphi_1 \leq \varphi_1^*$; $\varphi_2^* = \pi$; $\varphi_3^* = \pi$. The introduction of a limitation on angle φ_1 means that movement of link SE1 (Figure 13) over the sphere is limited by the solid angle formed by the rotation of the straight line SE1 around axis OO, which it interesects at angle φ_1^*. Now the space around point S does not possess identical properties along any radius-vector R, so let us investigate the individual regions of the space serviced by the manipulator. The working space can be presented as consisting of two zones, in the first of which, zone A, the Θ distribution will be the same as for the ideal manipulator, but in the second, zone B, will change from 0 to 1. The function $\Theta = f(R)$ is extremely complex.

/13

The total manipulator working space is limited by two concentric spheres with radii R_{max} and R_{min}, and part of the surface of the torus joining them. Figure 13 shows the cross section of the working space in the form of a plane passing through the OO axis.

Let us examine the distribution of service zones in the area delimited by lines DmEE1. We will select the coordinates of the points here in a polar coordinate system, (r), with center in point E1. We note that angle ϑ increases in this zone with movement of the tongs (point T) from the periphery to point E1. Because they are maneuverable, the tongs can rotate around axis E1T as well, so angle ϑ can characterize the service factor. Thus,

$$\Theta = \frac{l_2^2 - (r - l_3)^2}{4 r l_3}. \qquad (14)$$

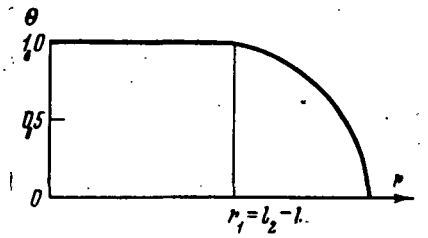

Figure 14.

We obtain the limiting value $r_1 = l_2 - l_3$ when $\Theta = 1$. Eq. (14) is valid when $r_1 \leq r \leq l_2 + l_3$, but when $r_1 \geq r \geq 0$ the service factor is constant and equals 1 (see Figure 14).

Considering the nature of the changes introduced in the distribution of the service zones by limitations on angles φ_1, φ_2, φ_3, it can be taken as an approximation that angle φ_3^* determines the maximum value of the service magnitude Θ, and that angles φ_1^* and φ_2^* influence the volume of space serviced by the manipulator, the service near the shoulder, and the boundaries of the space serviced.

4. Manipulator with limitations in all joints. Up to this point we have been considering manipulators with Class III spherical couples as joints. But manipulators use Class V couples for the most part and Class III spherical couples usually are replaced by a combination of three Class V couples, each of which has its own limitation in angle of rotation. These design features are reflected in the distribution of service zones.

Figure 15 shows a manipulator whose kinematic chain contains only Class V rotary kinematic couples. I is the frontal plane, II is the sagittal plane, and III is the base plane. The Mascot manipulator [3], for example, has this type of kinematic diagram. Its position in space can be determined by the generalized coordinates φ_i (i = 0, 1, ..., 5), determining movements in the

corresponding drives. Movements in each drive are limited, and the corresponding limiting values of the angles, as before, are designated by φ_i^*.

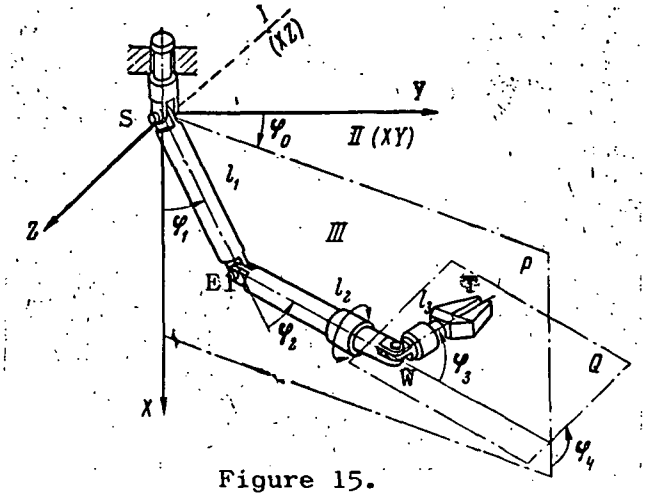

Figure 15.

/14

We will act in a manner similar to that preceding, wherein we replace the tongs with a ball joint located at some point T in the working space with coordinates (X_T, Y_T, Z_T). We obtain a three-dimensional arrangement with two degrees of freedom (rotation of link l_3 relative to its longitudinal axis is not considered). Movement will cause point W to move over the surface of a sphere with radius l_3 and center in point T. The task of determining Θ involves finding the spatial angle formed by the set of positions l_3, permitted by limitations φ_i^*.

Bear in mind that when the position of the tongs, T (X_T, Y_T, Z_T) is fixed, the wrist, W (X_W, Y_W, Z_W), and elbow, E1 (X_{E1}, Y_{E1}, Z_{E1}) can occupy two different positions. Both positions therefore must be checked from the point of view of satisfying limitations φ_i^*.

The coordinates of points T and W are set by the assigned position of the tongs, and angle φ_0, formed by the base plane, P (in which the shoulder, elbow, and wrist lie), and the Y-axis, is determined (Figure 15)

$$\varphi_0 = \operatorname{arctg} \frac{Z_3}{Y_3}.$$

Let us find angles φ_1 and φ_2.

$$\varphi_2 = \pm \arccos \frac{1}{2l_1l_2}\left(\frac{Y_3^2}{\cos^2\varphi_0} + x_3^2 - l_1^2 - l_2^2\right).$$

We can use

to find φ_1, from whence

$$\frac{Y_3}{\cos\varphi_0} = l_1 \sin\varphi_1 + l_2 \sin(\varphi_1 + \varphi_2),$$

$$\sin\varphi_1 = \frac{AB \pm \sqrt{C^2(C^2+B^2-A^2)}}{B^2+C^2}.$$

$$A = \frac{Y_3}{\cos\varphi_0}; \quad B = l_1 + l_2\cos\varphi_2; \quad C = l_2\sin\varphi_2. \tag{15}$$

We will take it that angle φ_1 can change in the limits $-\pi/2 \le \varphi_1 \le \pi/2$. Eq. (15) then will yield two values for φ_1, with the negative value of φ_2 corresponding to the larger φ_1 value.

Let us measure the relative rotation of the axes of joints E1 and W by the angle, φ_4, between planes P and Q (the latter is determined by points E1, W, T), read in the direction from plane P counterclockwise toward plane Q looking from point W to point E1. Let us find the coordinates of the point E1 /15

$$X_{E1} = l_1\cos\varphi_1; \; Y_{E1} = l_1\sin\varphi_1\cos\varphi_0; \; Z_{E1} = l_1\sin\varphi_1\sin\varphi_0.$$

The plane P equation will be

$$A_1X + B_1Y + C_1Z + D_1 = 0.$$

Here

$$A_1 = 0; \; B_1 = -\sin\varphi_0; \; C_1 = \cos\varphi_0; \; D_1 = 0.$$

The equation of the plane passing through the coordinate origin and of parallel plane Q, is found by solving

$$\begin{cases} A_2X_{E1} + B_2Y_{E1} + C_2Z_{E1} = 0, \\ A_2X_W + B_2Y_W + C_2Z_W = 0, \\ A_2X_T + B_2Y_T + C_2Z_T = 0. \end{cases}$$

Now

$$\varphi_4 = \pm\arccos\frac{C_2\cos\varphi_0 - B_2\sin\varphi_0}{\sqrt{A_2^2+B_2^2+C_2^2}}.$$

The φ_4 limitations in manipulators usually are symmetrical, so the sign of φ_4 is not significant.

We determine angle φ_3, the flexure in the wrist, to be the angle between vectors $\overline{E1W}$ and $\overline{WT}$

$$\varphi_3 = \pm\arccos\frac{(X_T - X_W)(X_W - X_{E1}) + (Y_T - Y_W)(Y_W - Y_{E1}) + (Z_T - Z_W)(Z_W - Z_{E1})}{l_2l_3}.$$

Let us use the relationship

(16)

$$X_T = l_1\cos\varphi_1 + l_2\cos(\varphi_1+\varphi_2) + l_3\cos\varphi_3\cos(\varphi_1+\varphi_2) - l_3\sin$$
$$\times\cos\varphi_4\sin(\varphi_1+\varphi_2)$$

obtained from the vector equation $\bar{l}_1 + \bar{l}_2 + \bar{l}_3 = \overline{ST}$ to establish the sign of φ_3. The φ_3 value in identity (16) that reverses will be that sought.

The result will be the finding of the angle φ_i values. Comparing them with the φ_i^* limitations, we can reach a conclusion as to the reality ($\varphi_i \leq \varphi_i^*$), or unreality ($\varphi_i > \varphi_i^*$), of the manipulator configuration for a given position of link l_3.

We now change the position of point W, leaving point T in its former place, and we repeat all the operations. We thust can establish the outlines of the spatial angle at given point T formed by real positions of the manipulator. If the manipulator has maneuverability, the whole set of positions of the mechanism satisfying the limitations imposed must be verified.

A given algorithm was used to write a program and a "Minsk-22M" electronic digital computer was used to calculate the full service factor for a manipulator with seven degrees of freedom (Figure 15). A number of variants were checked in which the lengths of the links (Table 1), and the magnitudes of the limitations on the angle of relative rotation of the links (Table 2), were changed.

The following relationships, in addition to the full service factor (Θ), were calculated: (a) the number of points in the working space at which the tongs can be oriented in the positive direction along the X-axis to the total number of points in the working space ($\bar{\delta}_1$); (b) the number of points at which the tongs can be oriented in the positive direction along the Z-axis to the total number of points in the working space, ($\bar{\delta}_2$); (c) the number of points at which the tongs can be oriented in the positive direction along the X-axis as well as in the positive direction along the Z-axis to the total number of points in the working space ($\bar{\delta}_{12}$).

Calculations were made for 245 points lying in the plane of symmetry of the working space for all variants. 256 positions of link l_3 were checked at each point. Table 3 lists the results of the calculations corresponding to each of the combinations of variants in Tables 1 and 2. /16

As may be seen from Table 3, variant 2T is the most advantageous. The example cited shows that an evaluation of the kinematic properties of a manipulator based on the service factor, $\bar{\Theta}$, permits ready selection of the most advantageous design variant.

TABLE 1

Length of links	A	B	C
l_1	98	88	108
l_2	83	93	73
l_3	25,5	25,5	25,5

TABLE 2

Limitation	1	2	3
φ_1	+45 −90	+45 −90	±90 ±90
φ_2	+135 0	+135 0	±90
φ_3	±90	+150 −30	±90
φ_4	±90	±90	±90

TABLE 3

Link length variants	1	2	3
A	$\bar{\theta} = 0,569$	$\bar{\theta} = 0,701$	$\bar{\theta} = 0,403$
	$\bar{\delta}_1 = 0,885$	$\bar{\delta}_1 = 0,889$	$\bar{\delta}_1 = 0,567$
	$\bar{\delta}_2 = 0,624$	$\bar{\delta}_2 = 0,710$	$\bar{\delta}_2 = 0,412$
	$\bar{\delta}_{12} = 0,546$	$\bar{\delta}_{12} = 0,608$	$\bar{\delta}_{12} = 0,241$
B	$\bar{\theta} = 0,498$	$\bar{\theta} = 0,675$	$\bar{\theta} = 0,374$
	$\bar{\delta}_1 = 0,844$	$\bar{\delta}_1 = 0,820$	$\bar{\delta}_1 = 0,567$
	$\bar{\delta}_2 = 0,575$	$\bar{\delta}_2 = 0,685$	$\bar{\delta}_2 = 0,396$
	$\bar{\delta}_{12} = 0,489$	$\bar{\delta}_{12} = 0,534$	$\bar{\delta}_{12} = 0,245$
C	$\bar{\theta} = 0,628$	$\bar{\theta} = 0,726$	$\bar{\theta} = 0,414$
	$\bar{\delta}_1 = 0,930$	$\bar{\delta}_1 = 0,922$	$\bar{\delta}_1 = 0,371$
	$\bar{\delta}_2 = 0,673$	$\bar{\delta}_2 = 0,722$	$\bar{\delta}_2 = 0,371$
	$\bar{\delta}_{12} = 0,618$	$\bar{\delta}_{12} = 0,649$	$\bar{\delta}_{12} = 0,371$

REFERENCES

1. Kobrinskiy, A. Ye., Stepanenko, Yu. A., "Some Problems of Manipulator Theory," V sb. Mekhanika mashin [In collection: Mechanics of Machines], No. 7-8, "Nauka" Press, 1967.

2. Artobolevskiy, I. I., Teoriya mekhanizmov [Theory of Mechanisms], "Nauka" Press, 1967.

3. Mancini, C., Roncaglia, F., "The C.N.E.N. Electric Servomanipulator Mascot," Alta frequenza, No. 6, 1963, p. 32.